Structural and Vibrational Assignment of *p*-Methoxyphenethylamine Conformers

Iñigo Unamuno, Jose A. Fernández, Asier Longarte, and Fernando Castaño*

Departamento de Química-Física, Facultad de Ciencias, Universidad del País Vasco, Apartado 644, 48080 Bilbao, Spain

Received: December 10, 1999; In Final Form: February 7, 2000

A combined wide range of laser spectroscopic techniques and computational quantum chemistry are used to investigate conformer landscapes of large substituted aromatic molecules. The spectroscopic techniques include laser-induced fluorescence (LIF), high-resolution LIF, resonance-enhanced multiphoton ionization (REMPI) with mass detection, two-color resonance ionization with mass detection (R2PI), laser dispersed emission (DE), and ion-dip hole burning (HB). These techniques are balanced with extensive ab initio DFT calculations at the B3LYP/6-31+G* and B3LYP/6-311+G* levels. These methods have been applied to investigate the nine possible conformations of the *p*−methoxyphenethylamine (MPEA) neurotransmitter molecule. Even when all the spectroscopic techniques play important roles, two color ionization energy (IE) threshold determinations have proven to be especially useful in the study. The gauche and anti conformers exhibit different ionization energy values, and even the amino hydrogen orientation influences their energies. The results allow the unequivocal identification of seven conformer structures which are further confirmed by the assignment of their vibrational spectra. A discussion on the intramolecular interactions, including the N−H···π hydrogen bonding correlation with the molecular stability in the light of the theoretical and experimental results, is also presented.

I. Introduction

Neurotransmitter molecules are chemical messengers from the nervous presynaptic cells to the postsynaptic cell receptors; the changes associated with the process permit the opening of Ca^{2+} ion channels to the ionic valve. A considerable number of synapsis actions are carried out by neurotransmitters. Although the cholinergic synapsis is the best known, there are other action types conducted by benzene derivatives, such as the cathecolamine, dopamine, and amphetamine families—referred to henceforth as *aromatic neurotransmitters*—that play an important role in the nervous transmission.[1]

The structure of the simple *aromatic neurotransmitters* family consists of a hydroxy, amino, or other substituted aromatic ring with an alkylamine tail; this combination provides the biological activity and at the same time gives rise to flexible structures and a rich variety of conformers. The very existence of many conformers, along with the accessibility of their chromophore (320−280 nm) by standard laser tunable techniques and a vapor pressure suitable for use in adiabatic expansions—cooling the vibrational and rotational degrees of freedom, and simplifying the otherwise overcrowded spectra—make these molecules particularly attractive in modern applied spectroscopy.

The molecular conformers arise from the internal rotation around the $C_\alpha-C_\beta$ bond (standard nomenclature; cf. later, in Figure 2), and the possible orientations adopted by the amino group lead to pairs of gauche and anti conformers, all with close 0_0^0 transitions and very similar spectra. From the chemical point of view, these molecules are interesting examples of conformations stabilized by intramolecular interactions (between the π-system electron density and the amino group). These interactions are found in many biomolecules and are considered, together with the hydrogen bond, to play an important role in the formation of the secondary and tertiary structures of large biological molecules, including proteins and DNA. The simplest member of the aromatic (benzene) *neurotransmitter* family is the phenethylamine (PEA); attaching OH or O(Me) substituents to the aromatic ring or methyl groups to the amino side, other molecules of the family are obtained, in particular tyramine and *p*-methoxyphenethylamine (MPEA) (Figure 1). The spectroscopy and photophysics of these molecules are rich and not yet well-understood.

The best-studied neurotransmitter, in spectroscopic parlance, is the PEA molecule, first analyzed in a supersonic expansion by Martinez III et al.[2] Its LIF, disperse fluorescence emission, and pressure-dependent studies, combined with the results of previous works on *n*-propylbenzenes,[3] led to the identification of four PEA conformers, six conformers of tyramine and tryptamine,[4−6] and seven conformers of MPEA.[7,8] Martinez III et al.[2] also were able to identify groups of gauche and trans conformers for the two simplest members of the family (PEA and tyramine). Nevertheless, these authors were unable to justify the existence of seven MPEA conformers and could identify only four of them as pairs of gauche conformers and a fifth one as anti. The geometric structures proposed for the conformers must be regarded as tentative.

In a recent paper, Godfrey et al.[9] used microwave spectroscopy to identify the two strongest bands of the PEA spectrum as belonging to isomers in a folded (gauche) configuration. By comparing the experimental results with ab initio calculations, they concluded that folded configurations are favored over the extended, or anti, conformers, due to the extra stabilization provided by the N−H···π interaction. These authors were unable to detect the other two conformers previously identified by Martinez III et al.,[4] probably because of the conformers' low concentration in the beam and the sensitivity of the method. In a combined LIF and HB study, Sun and Bernstein[10] found an

* To whom correspondence should be addressed: E-mail, qfpcaalf@lg.ehu.es; fax, ++ 34 94 464 85 00; phone, ++ 34 94 601 2533.

10.1021/jp9943528 CCC: $19.00
Published on Web 04/19/2000

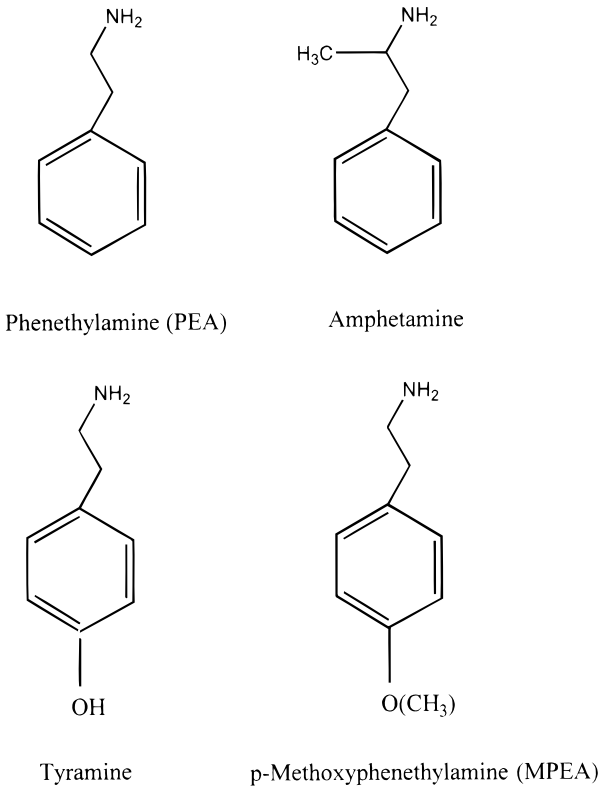

Figure 1. Molecular structure of a few significant neurotransmitter messengers of the *p*-methoxyphenethylamine (MPEA) family.

extra-low-intensity origin band that was assigned to the fifth conformer. Recently, Dickinson et al.[11] reassigned that fifth origin band to a monohydrated PEA complex. As already noted, even the spectroscopy of the simplest member of the aromatic family is not well-established, and certainly, more complex members, like tyramine, dopamine, and MPEA, require further studies. Conformation studies on other benzene derivatives of biological interest, using theoretical[12] and laser-based spectroscopy background, have also been reported.[13−15]

In the present work, LIF, REMPI, high-resolution LIF and REMPI, R2PI, ion-dip HB, DE study, and the crucial interplay with ab initio calculations using DFT and different basis sets have been applied to the MPEA molecule to identify its conformers. The analysis of both sets of theoretical and experimental results have led to the unequivocal identification of seven conformers, completed with the assignation of their vibrational spectra by comparison with the calculated frequencies. To the best of our knowledge, this is the first time that a considerable number of normal vibrational modes are assigned for a neurotransmitter molecule. A discussion on the significance of the N−H···π interaction in the molecular geometry stabilization is presented in the light of the results obtained.

II. Procedures

A. Experimental. The experimental setup used to carry out the present study has been described elsewhere,[16] and only a succinct account will be provided here. The system is built around either one frequency-doubled excitation dye laser (LIF) or two pump/probe frequency-doubled and synchronized dye lasers, and two vacuum chambers, designed for radiation detection and for mass selective detection studies, respectively. The resulting signal is routed to suitable oscilloscopes, electronics, and computer facilities for analysis and storage.

In the mass-resolved experiments, an R. M. Jordan stainless steel valve was employed, fed with He as buffer gas, at a stagnation pressure of 2−5 bar and seeded with MPEA in a flowing mixture. The supersonic expansion itself is effected inside an R. M. Jordan TOF chamber, kept at an average pressure of 6×10^{-6} mbar. Its central part—where the beam is well-characterized—is passed through an 0.8-mm ϕ skimmer to get a uniform pulsed beam to further carry out the ionization by pulsed lasers, and also to measure the TOF of the ions from creation to arrival at the microchannel plate (MCP) detector. The molecular expansion is crossed at right angles by an XeCl-excimer/dye laser beam, tuned at the MPEA first electronic transition, which pumps and ionizes the molecules by a 1 + 1 absorption process. In the R2PI experiment, the first dye laser pumps the molecule to its first electronic excited state. Later, after an appropriate delay, the second laser, in a counterpropagating coaxial geometry, ionizes the species with the minimum energy excess. The ion-dip HB spectrum is recorded by setting the probe-delayed laser to a predetermined conformer absorption and further scanning the pump laser in the region of interest. When the pump laser is tuned to a band of the same conformer, it depletes its ground-state population, and the probe signal diminishes. In any other case—including the pumping to bands leading to the ionization of other conformers—the probe signal remains unchanged.

Ionized species are extracted by suitable electric fields and flight to the MCP detector. The delayed arrival time is inversely proportional to the square root of the mass. The signal generated by the MCP is routed to a Tektronix 2430A digital oscilloscope, where it is integrated, averaged, and sent to a personal computer for further analysis and storage. High-resolution pulsed REMPI experiments were carried out by placing an Etalon in the excimer pumped-dye laser oscillator; the resolution in the visible region was measured to be 0.035 cm^{-1}.

In the LIF and DE experiments, the TOF chamber was substituted by a stainless-steel cylinder having four appropriated viewports and a pulsed Iota One valve (General Valve) attached to the cylinder cover. The emitted light following laser excitation was conveniently focused by aspherical lenses either directly onto a side-on photomultiplier (R928 Hamamatsu) or into the slits of a 1-m F/7.8 monochromator (Spex model 1000M) and detected by either an R928 Hamamatsu or a 9830 EMI photomultiplier backed by suitable electronics and data handling.

Laser tuning was effected with the aid of either coumarine 540 or fluoresceine 548 dyes (Exciton) and monitored in real time by a Fizeau wavelength meter (New Focus model 7711). The suitable MPEA vapor pressure and concentration to perform the experiments was achieved by heating the sample at 100 °C and the pulsed valve at ca. 70 °C.

B. Ab Initio Calculations. Ab initio calculations were conducted at several theory levels and with a variety of basis sets. Because of the large size of the system (82 electrons), the theory level and basis set must be carefully chosen. B3LYP is known to yield very accurate geometries and excellent vibrational frequencies at reasonable CPU times.[17] However, it is also known to be less successful in describing interactions dominated by dispersion forces. The main interaction in the MPEA (N−H···π) structure is not clearly dominated by any of the H-bond, dispersion, or electrostatic intermolecular forces. Because of the hindrance imposed by the molecular geometry, the amino hydrogen is too far apart from the aromatic ring to consider the interaction as a pure H-bond. However, the distance is not far enough to assume that only the pure dispersive interaction dominates. As a result, one concludes that the

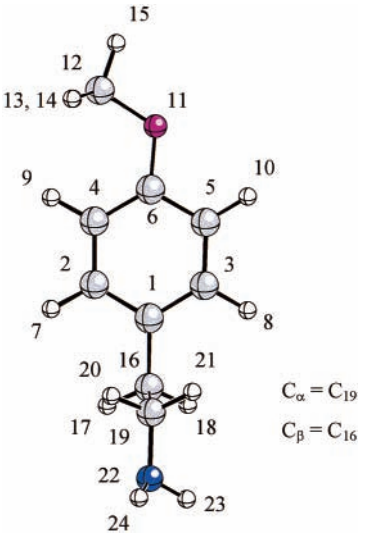

Figure 2. Molecular structure numeration of the *p*-methoxyphenethylamine atoms as used in the computations and referred to in the discussion.

dispersion forces are but one of the contributions to the N−H···π interaction, and not even the largest contribution. Studies of other groups suggest the use of MP2 for the same type of molecular systems (as in PEA or *p*-tyrosol).[13] MP2 is probably the best alternative, but it means an increase in CPU time and poor vibrational frequencies compared to those provided by the B3LYP method.[17] Because the frequency calculation is a key point in the conformers identification, we will use B3LYP to conduct the calculations presented in the paper.

In the geometry optimization process, no constraints were imposed on the structures. Geometries, vibrational frequencies, and zero-point energies (ZPEs) were calculated at the B3LYP/6-31+G* level. A single-point calculation on the optimized geometries was conducted at the B3LYP/6-311+G* level to improve the computed energies. All these calculations were conducted with the Gaussian 98W suite.[18]

III. Results

A. Geometry Calculations. MPEA conformers are generated by rotation around two bonds: $C_\alpha-C_\beta$ and $C_\alpha-N$ (see Figure 2). The former leads to three different orientations of the NH_2 group with respect to the O(Me) substituent, whereas rotation around the $C_\alpha-N$ bond leads to three different orientations of the amino hydrogens. The nine possible conformers generated in this way (referred to hereinafter as CF1 to CF9) are shown in Figure 3, and their structural parameters are described in Tables 1 and 2. Table 1 shows the bond distances and bond and dihedral angles of conformers 1 and 8 (CF1 and CF8)—the most stable anti and gauche conformers, according to the calculations—and Table 2 depicts the largest structural parameter changes among the nine conformers and also the calculated binding energies. Geometry, vibrational frequencies, and ZPE values were calculated at the B3LYP/6-31+G* level, while energies were also recomputed (without further geometry optimization) at the B3LYP/6-311+G* level. The good agreement between experimental and calculated vibrational values confirms that the calculated ZPE can be used to correct the energies obtained at the B3LYP/6-311+G* level.

According to the data shown in Table 1, most conformer bond distances are marginally different, and only three bond distances are significantly affected by the conformational change: $C_\alpha-C_\beta$ ($C_{19}-C_{16}$), $H_{17}-C_\beta$, and $C_\beta-H_{18}$. Paradoxically, the $H_{23}-N_{22}$ and $N_{22}-H_{24}$ bond distances remain unaffected, despite the fact that in some conformers the interaction between the amino hydrogens and the C_α is much larger than in others.

The structural parameters most affected by the conformational change are those of the alkylic moiety, reflecting the bonds' and bond angles' stress to enhance the N−H···π interaction (where the N−H···π length is defined as the distance between the "internal" NH_2 H and the nearest ring's carbon), whereas the aromatic ring angles remain unchanged. Particularly large is the adjustment in the $C_\alpha-C_\beta-N$ angle, which becomes smaller when the amino hydrogens are rotated from the "down" position to a "side" configuration (e.g., from 116.0° for CF1 to 110.7° for CF2).

It is worth noting, and is expected from the molecular asymmetry, that the $C_1-C_\alpha-C_\beta$ and the benzene ring planes are not perpendicular but form a characteristic angle for each conformer in order to balance the amino hydrogens and the N−H···π aromatic ring interaction. This interaction is higher in the CF5 and CF8 structures, as is readily seen by the smaller calculated hydrogen bond distance of the N−H···π (2.769 Å for CF5 and 2.759 Å for CF8). CF1 also has a $C_1-C_\alpha-C_\beta$ plane nonorthogonal to the aromatic ring (cf. Table 1), but the separation from perpendicularity in this conformer is due to a modulation of the aromatic ring binding distances and angles caused by the O(Me) group.

All calculations point to CF8 as the most stable structure and to CF6 and CF9 as the less energetically favorable conformers. Nevertheless, the relative stability of the other conformers varies slightly with the basis set used and the introduction of ZPE corrections. On the other hand, the BSSE correction does not seem to affect the relative stability of the nine calculated conformers. At the B3LYP/6-31+G* level, all the folded (gauche) conformers except two, CF6 and CF9, are more stable than CF1, which is the most stable extended anti conformer. When ZPE is taken into account, the three anti conformers' stability comes closer to that of CF8, and even CF1 becomes the second most stable conformer, a mere 7 cm^{-1} less stable than CF8. At this level and with the ZPE correction, the N−H···π interaction does not seem to be large enough to compensate for the C_α-H···H−N and C_α-H···H− C_β destabilizing interactions.

In the computations with the larger basis set (6-311+G*), the difference between conformers' stability increases. It seems as though larger basis sets, with electrons spreading far apart from the nuclei, are required to account for long-range interactions. Here and again, the ZPE correction changes the CF1, CF4, CF5, and CF7 relative stability sequence. Despite the differences in the absolute values of the conformers' relative stability, the calculations show that CF6 and CF9 are more than 500 cm^{-1} less stable than CF8, an energy large enough to make their beam concentrations too small to be detected.

B. Experimental Results. In Figure 4 the bare MPEA molecule LIF and REMPI spectra and the MPEA$(H_2O)_1$ REMPI spectrum in the 35 500 to 36 000 region are presented. The LIF spectrum is in good agreement with the spectrum previously reported by Martinez III et al.,[2] where the peaks labeled A to G were identified as the origin bands of seven different conformers. The REMPI spectrum shows a large number of peaks in the ~35 700 cm^{-1} region due, in part, to the MPEA-$(H_2O)_1$ complex fragmentation. Indeed, many of these peaks match those of the MPEA$(H_2O)_1$ REMPI spectrum. An analysis of the monohydrated MPEA complex is under way in our laboratory.

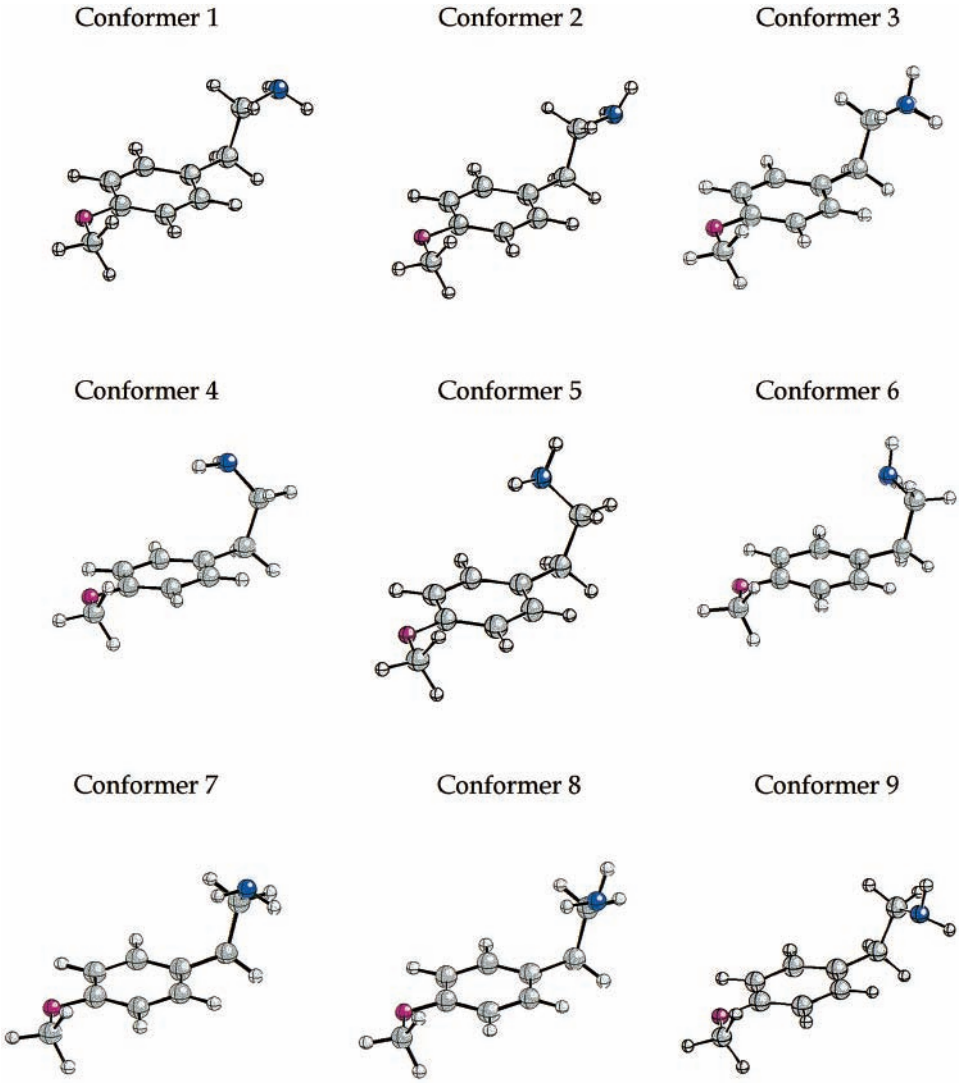

Figure 3. B3LYP/6-31G* optimized geometry of the nine *p*-methoxyphenethylamine conformers. Conformers are referred to as CF followed by an identification number. The top row shows the molecular structure drawings of the extended (anti) MPEA conformers (in trans, trans, and cis sequence, beginning from the left), and the medium and bottom rows depict the three trans and the three cis folded (gauche) conformers, respectively.

To identify the conformer vibrational bands and to examine the existence of previously undetected conformers, an ion-dip HB study was carried out in the region 35 500−36 800 cm^{-1}, setting the probe laser at the conformer origin bands (labeled A to G in Figure 4). In Figure 5 and as an illustration, the ion-dip HB spectra in the 35 500−35 900 cm^{-1} region are presented. As can be observed, the seven peaks have independent origin bands and thus are associated to different conformers. In addition, the peaks due to water complexes do not correlate with any bare molecule origin band. On the contrary, all the significant peaks not due to water complexes correlate with one of the seven origin bands. Therefore, one concludes that the previous assignment based on laser power-dependence evidence is correct and that no other conformers are present.

To correlate the experimental 0_0^0 origin bands with those calculated for the conformers, the ionization energy thresholds (IE) for the seven conformer origin bands were determined. Figure 6 shows the traces of the signal intensity versus the ionization laser wavenumber, and Table 3 presents the IE obtained. The traces depicted in Figure 6 rise slowly from threshold compared with those of common bare molecules, resembling the traces found in van der Waals complexes, which usually indicate dramatic geometry changes in the transition from the molecular excited state to the ion.[19] The extraction of one electron from the aromatic ring strongly perturbs the N−H···π interaction, leading to a reorientation of the whole molecular structure. The Franck−Condon factors for the $MPEA^+ \leftarrow MPEA^*$ transitions are therefore very unfavorable, leading to a slow ramp for the ionization trace. Accordingly, the steepest IE corresponds to the E band, already assigned to CF1, the conformer where there is no HN−H···π interaction; therefore, less molecular reorganization is expected from S_1 to I_0 states.

The seven conformers' 0_0^0 bands in Figure 6 appear to be grouped: four of them (labeled A−D and already assigned as gauche) appear in the set to the blue, whereas the other three (E−G) are to the red. The four gauche conformers can, in addition, also be grouped in pairs: the A/C pair has a higher IE than that for B/D pair. That is, gauche−cis conformers with cis configuration relative to the O(Me) group exhibit similar IE and are shifted with respect to those from the gauche−trans pair. The amino hydrogens' position is possibly responsible for the subtle difference in the IE within the gauche-cis and gauche-trans conformer pairs. This observation makes the assignment easier, but does not yet allow us to identify the cis or trans isomer pairs (A−C or B−D).

The F and G ionization traces of the $I_0 \leftarrow S_1$ transitions are slightly shifted to the red of the E $I_0 \leftarrow S_1$ transition (previously

TABLE 1: Structural Parameters of CF1 and CF8 of MPEA Conformers (see text and Figure 3), Calculated at the B3LYP/6-31+G* Level

bond distance	conformer CF1	conformer CF8	angles	conformer CF1	conformer CF8
C_1-C_2	1.398	1.399	$C_2-C_1-C_3$	117.4	117.4
C_1-C_3	1.406	1.407	$C_1-C_2-C_4$	122.0	121.9
C_2-C_4	1.401	1.402	$C_1-C_3-C_5$	121.6	121.6
C_3-C_5	1.391	1.391	$C_4-C_6-C_5$	119.5	119.4
C_4-C_6	1.400	1.399	$C_6-O_{11}-C_{12}$	118.5	118.4
C_5-C_6	1.403	1.404	$O_{11}-C_{12}-H_{13}$	111.4	113.6
C_2-H_7	1.089	1.088	$O_{11}-C_{12}-H_{15}$	105.8	105.8
C_3-H_8	1.089	1.089	$C_1-C_{16}-C_{19}$	113.1	113.6
C_4-H_9	1.085	1.085	$H_{17}-C_{16}-H_{18}$	106.5	107.3
C_5-H_{10}	1.086	1.086	$H_{20}-C_{19}-H_{21}$	106.3	107.2
C_6-O_{11}	1.369	1.370	$C_{16}-C_{19}-N_{22}$	116.	111.0
$O_{11}-C_{12}$	1.420	1.421	$H_{23}-N_{22}-H_{24}$	107.0	107.0
$C_{12}-H_{13}$	1.098	1.098	$C_8-C_1-C_{16}-C_{19}$[b]	88.0	80.7
$C_{12}-H_{15}$	1.092	1.092	$C_1-C_{16}-C_{19}-N_{22}$[b]	180.1	64.3
C_1-C_{16}	1.513	1.515	$H_{17}-C_{16}-C_1-C_2$[b]	31.5	23.4
$C_{16}-H_{17}$	1.099	1.097			
$C_{16}-H_{18}$	1.099	1.098			
$C_{16}-C_{19}$	1.549	1.540			
$C_{19}-H_{20}$	1.097	1.105			
$C_{19}-H_{21}$	1.097	1.097			
$C_{19}-N_{22}$	1.464	1.468			
$N_{22}-H_{23}$	1.018	1.019			
$N_{22}-H_{24}$	1.018	1.018			

[a] Angles are given in degrees, distances in Å. $C_{16}\equiv C_\beta$ and $C_{19}\equiv C_\alpha$ (see Figure 2). [b] Dihedral angle.

identified as anti), but very close to it. This pattern indicates both that F and G bands are also associated to anti conformers and that, as happens for gauche conformers, their amino hydrogens' relative orientation originates a faint difference in the IE with respect to the E band conformer, where the hydrogens are pointing down and to the front, thereby precluding any chances of cis and trans interactions with the O(Me) group. In consequence, one may safely assign the E-labeled band to the CF1 structure.

Once the ionization energy is determined, it is possible to record the two-color R2PI spectrum. Figure 7 depicts the spectrum obtained by setting the ionization laser S_1-S_0 band at 29 239 cm^{-1}. When Figure 7 is compared with Figure 4b, two differences are readily observed: the number of peaks due to MPEA$(H_2O)_1$ complexes decreases, and the features around 36 400 cm^{-1} are now less intense. This last observation probably is due to laser power saturation in the one-color spectrum.

So far, the information presented here is related to the MPEA S_1 excited state. To obtain information about the ground state, the conformers' dispersed fluorescence emission spectra have been analyzed. A comparison between the calculated vibrational frequencies and the experimental bands' positions also is of considerable help in the conformers' assignment. Figure 8 shows the dispersed emission spectra obtained at 2-bar stagnation pressure, and monochromator slits of 150 μm corresponding to a resolution ca. 12 cm^{-1}. The spectra depicted in Figure 8 show intense peaks around ~800 cm^{-1} to the red of their origin band and correspond to intense features in the REMPI spectrum. The appearance of these peaks as doublets or singlets does not correlate with any possible conformer assignment and has no easy explanation. The set of spectra also shows some vibrational activity around 1300 cm^{-1} and 1600 cm^{-1} and becomes a continuum over 1800 cm^{-1}. A comparison between ground and excited state and calculated vibrational frequencies is presented in the next section, after the discussion of the final assignment.

IV. Discussion

A. Conformer Identification. The early works based on LIF, DE, and chemical criteria identified the seven MPEA conformers as two pair of gauche (A, B and C, D) and one anti (E), and left the other two conformers unassigned.[2] There were no chances at that time to identify the conformers' geometry. The ionization energies justify this assignment and offer additional information: the F and G band conformers are identified as anti. One may regard the system as follows: the CF1 structure has the NH_2 group far apart from the aromatic ring, resulting in a small NH$\cdots\pi$ interaction. The other conformers have weak or strong interactions with the aromatic ring and with the O(Me) group, leading to red-shifted $S_1 \leftarrow S_0$ transitions with respect to CF1 for the gauche conformers and to small blue-shifted $S_1 \leftarrow S_0$ transitions for the anti conformers. The latter exhibit smaller shifts as the interaction is produced between the two distant substituent moieties of the aromatic ring.

The same pattern is observed for the ionization energy: if one considers the CF1 threshold as "zero-shifted", then the interaction between the other two anti conformers shifts their $I_0 \leftarrow S_1$ transition energy to the red, opposite to the blue shift exhibited by the $S_1 \leftarrow S_0$ transition (where I_0, stand by the lower ionization state). The interaction produced in the gauche conformers shifts their thresholds to the blue and groups them in cis−trans conformer pairs, with the same rotation around the $C_\alpha-N$ bond. While the cis−trans interaction produces a significant shift both in the conformer $S_1 \leftarrow S_0$ and in the $I_0 \leftarrow S_1$ transitions, it seems the orientation of the amino hydrogens (pointing down or to one side) groups the conformers' $S_1 \leftarrow S_0$ origin bands into pairs separated by 44 cm^{-1}, but has a smaller influence on the $I_0 \leftarrow S_1$ transition energy.

The assignment of the gauche structures is a difficult task. An assignment based on purely energetic arguments has proven useless, because the interaction between the amino group and the aromatic ring modifies the molecule oscillator strength in a different way for each conformer, affecting the intensity of the 0_0^0 transitions. In addition, differences in the conformers' Franck−Condon factors, in S_1 lifetimes; ionization cross section at the chosen wavelength; and partial relaxation between the conformers in the expansion may also influence each conformer to a different extent. As there are six calculated structures and only four experimental conformers, we need to rule out two theoretical possibilities. Based on energy calculations, the CF6 and CF9 structures are the less stable conformers; their energy differences are large enough to have negligible population at the beam expansion vibrational temperature (a few tens K) and, consequently, not be detected. The relative stability of the other isomers cannot be used as a guideline for the assignment, because their energy differences are smaller and because each conformer shows a specific interaction with the aromatic ring of different magnitude. This interaction can also affect the transition dipolar moment and, therefore, the oscillator strength.

The comparison of experimental and calculated vibrational frequencies may also help to identify cis−gauche and trans−gauche conformers, although most vibrational frequencies are very close in the whole set of conformers. The biggest differences in vibrational frequencies, which therefore are useful in the assignment, are the lowest ones, which correspond to the torsion around the C_1-C_β bond. Obviously, the strength of the N−H$\cdots\pi$ interaction has a big influence on this torsional vibration. Bearing in mind that peaks (A, B) and (C, D) correspond to pairs of gauche conformers with the same orientation of the amino hydrogens, and different relative orientation of the NH_2 group, the comparison of calculated ν_1

TABLE 2: Comparison of Some Bonds, Bond Angles, and Dihedral Angles of the Nine MPEA Conformers[a]

	conformer								
	1	2	3	4	5	6	7	8	9
$C_{16}-C_{19}$	1.549	1.539	1.539	1.551	1.540	1.546	1.551	1.540	1.543
$C_{19}-H_{20}$	1.097	1.104	1.097	1.098	1.097	1.104	1.098	1.105	1.096
$C_{19}-H_{21}$	1.097	1.097	1.104	1.097	1.105	1.096	1.097	1.097	1.104
$C_1-C_{16}-C_{19}$	113.1	112.9	113.0	113.9	113.7	115.1	113.8	113.6	114.9
$H_{17}-C_{16}-H_{18}$	106.5	106.6	106.6	106.5	107.3	106.1	106.6	107.3	106.1
$H_{20}-C_{19}-H_{21}$	106.3	106.8	106.8	106.6	107.1	107.0	106.6	107.2	107.0
$C_{16}-C_{19}-N_{22}$	116.	110.7	110.4	116.9	111.1	111.5	116.8	111.0	111.4
$H_{23}-N_{22}-H_{24}$	107.0	106.9	106.9	107.0	107.0	106.9	107.0	107.0	116.8
$C_8-C_1-C_{16}-C_{19}$[b]	88.0	85.4	85.9	96.6	95.0	72.8	80.1	80.7	104.6
$C_1-C_{16}-C_{19}-N_{22}$[b]	180.1	179.3	182.8	297.7	295.8	286.6	62.5	64.3	73.1
$H_{17}-C_{16}-C_1-C_2$[b]	31.5	28.3	28.9	39.6	37.4	14.5	24.0	23.4	47.9
$C_{ring}\cdots HN$				2.850	2.769		2.841	2.759	
ΔE (cm^{-1})									
B3LYP/6-31+G*	79	147	152	81	50	590	59	0	592
B3LYP/6-31+G*-ZPE	7	70	86	61	34	551	49	0	520
B3LYP/6-311+G*	116	142	148	93	52	576	69	0	557
B3LYP/6-311+G*-ZPE	44	65	82	73	36	537	59	0	485

[a] The calculated binding energies (in cm^{-1}) relative to the most stable conformer are also shown. Note the structural differences between the most stable conformers, CF1 and CF8, and the other conformers. [b] Dihedral angles.

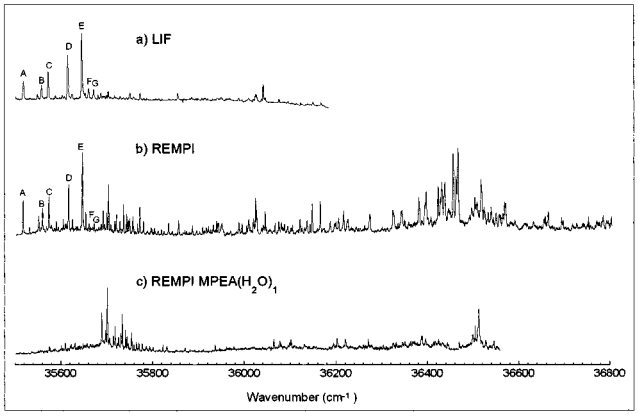

Figure 4. Laser-induced fluorescence spectrum, a), and one-photon mass-selected REMPI spectrum, b), of the *p*-methoxyphenethylamine molecule in a supersonic expansion. Bands indicated as A, B... to G correspond to the seven identified conformers. One-photon mass-selected REMPI spectrum of the monohydrated *p*-methoxyphenethylamine complex c) is also shown for comparison and discussion purposes.

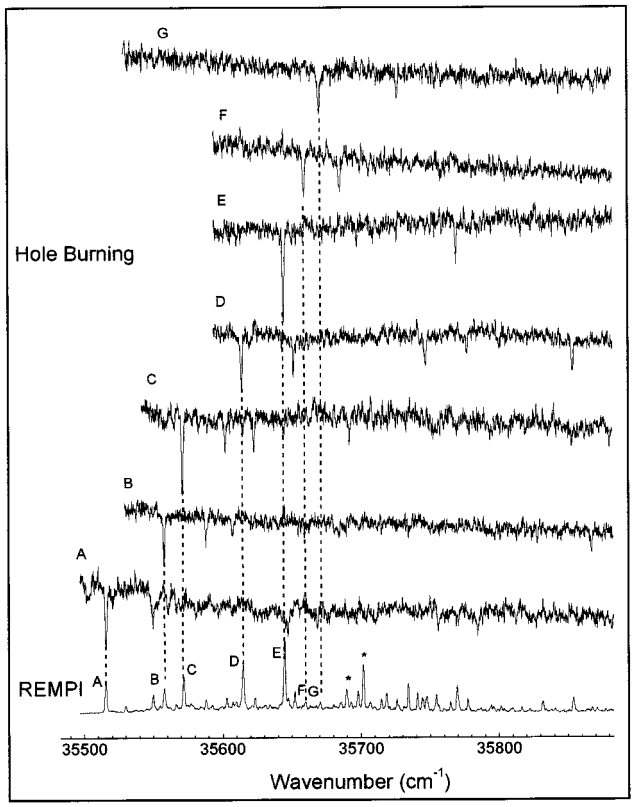

Figure 5. Ion-dip hole-burning spectra recorded with the probe laser frequency centered on A, B... and G conformer peaks. The REMPI spectrum and the dotted lines are guides for the conformer vibrational bands' identification. Bands marked with stars in the REMPI spectrum belong to the monohydrated *p*-methoxyphenethylamine complex.

with the first vibration in the emission spectrum leads us to assign A band as CF8, B as CF5, C as CF7, and D as CF4. Table 4 summarizes the experimental (emission and excitation) and the calculated frequencies for the assigned conformers.

The tentative assignment of the three anti conformers is based on subtle evidence. The comparison between the vibrational frequencies has proved useless; the $N-H\cdots\pi$ bond is very weak, and it seems that only the relative stability of the anti conformers can guide the assignment. Based on these considerations, one might expect the CF1 origin band to be more intense than that of the other two (Table 2). Accordingly, the E peak is more intense than that of either the F or G bands and, therefore, one assigns the E peak to CF1 structure. The isomerization barrier from CF2 or CF3 to CF1 probably is small enough to allow MPEA to adopt the most energetically favorable structure during the cooling process, resulting in a relatively larger population of CF1 than of either CF2 or CF3. The same argument does not apply to the gauche conformers, for which the isomerization barriers are much larger.

The assignment of F and G peaks to CF2 and CF3 structures can be based on two arguments: first, the most stable isomer should be associated with the higher peak, according to the above arguments, and thus the F peak is assigned to CF2 structure and the G peak to CF3. Second, the gauche−cis conformers' 0_0^0 bands exhibit a $S_1 \leftarrow S_0$ transition red-shifted with respect to the gauche-trans, and their ionization threshold is blue-shifted with respect to the trans partner (i.e. the CF8 0_0^0 origin, associated with the A peak, is red-shifted with respect to the CF5 one, associated with the B peak, and the CF8 ionization threshold is blue-shifted with respect to that of CF5). In the case of extended anti conformers, the interaction with the aromatic ring probably is due to the NH_2 dipole moment,

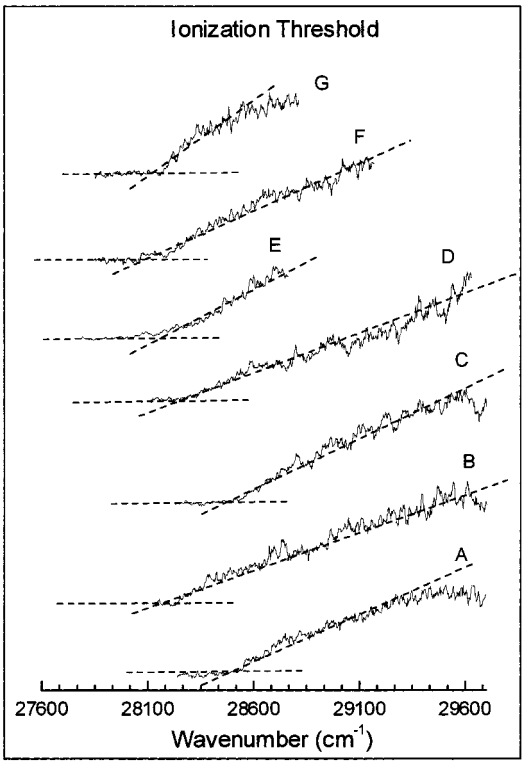

Figure 6. Ionization energy traces and thresholds of the *p*-methoxyphenethylamine conformers recorded by plotting the detector signal versus the laser ionization wavenumber near the $I_0 \leftarrow S_1$ transition. Traces are identified with the same letters A, B,... and G as the LIF and REMPI spectra conformers' bands. The pump laser was set to the specified conformer $S_1 \leftarrow S_0$ transition.

TABLE 3: 0_0^0 Transition Wavenumbers and Ionization Energy Thresholds for the MPEA Experimental Conformers

	origin						
	A	B	C	D	E	F	G
$S_1 \leftarrow S_0$	35 505	35 546	35 559	35 601	35 630	35 645	35 655
$I_0 \leftarrow S_1$	28 493	28 166	28 468	28 248	28 148	28 091	28 125
IT[a]	63 998	63 712	64 027	63 849	63 778	63 736	63 780

[a] Ionization energy threshold.

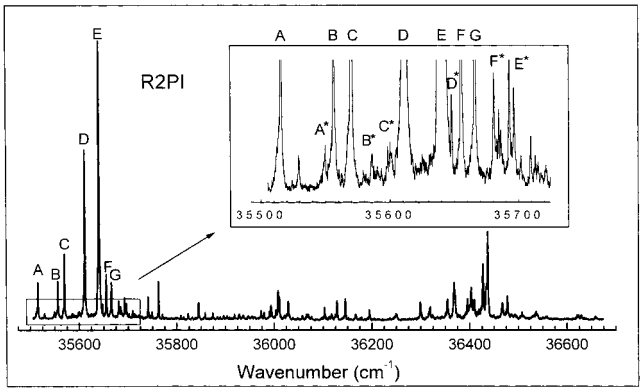

Figure 7. Mass-selected two-color R2PI spectrum of *p*-methoxyphenethylamine molecule in a supersonic beam, in the region of the $S_1 \leftarrow S_0$ origin band.

and CF2 could be considered as an anti−trans conformer because its NH_2 dipole moment is in a trans with respect to the O(Me) group. By analogy with the gauche conformers' behavior, the $S_1 \leftarrow S_0$ transition of CF2 should shift to the blue, and the $I_0 \leftarrow S_1$ should appear to the red of that of CF3, as observed.

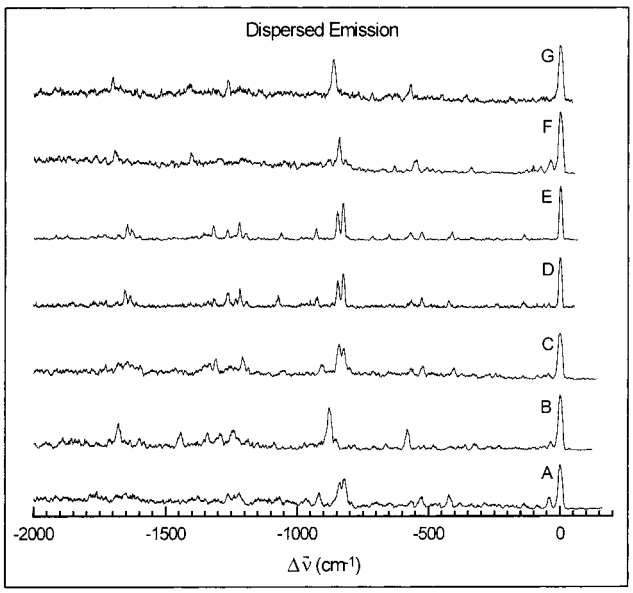

Figure 8. Dispersed fluorescence spectrum of *p*-methoxyphenethylamine molecule in a supersonic beam jet recorded by tuning the excitation laser on one of the seven conformer bands. The conformer bands are identified as from A to G matching the nomenclature used for LIF, REMPI, and R2PI spectra. FWMH resolution was of 12 cm^{-1}.

In consequence, the F peak is plausibly assigned to the CF2 structure and the G peak to the CF3.

B. Vibrational Assignments. Once the conformer peaks have been identified, it is feasible to assign their vibrational spectra, using the calculated vibrations at the B3LYP/6-31+G* level as a guideline. Table 4 shows the assignments proposed for the excitation and emission spectra of the gauche conformers, and Table 5 depicts the assignments for the three anti structures. The description of the vibrational modes appearing below the tables follows Wilson's conventions.[20] However, because of both the molecular asymmetry and the large size of the system, many vibrations are difficult to describe, in particular those involving the coupled movement of several parts or groups. For example, the CF8 ν_7 transition is a combination of the torsion around the $C_\alpha-C_\beta$ bond and the $Ph-O-CH_3$ group bending. For the sake of brevity, Table 4 presents only the description of the CF8 vibrational modes, as it is the most stable gauche conformer. The vibrational modes' sequence in other conformers may change with respect to that of CF8, though most of them remain in the same order. In the same way, the bottom of Table 5 presents a description of the vibrational modes for CF1, and the differences between it and the other two anti conformers are highlighted. Anti and gauche conformers have similar vibrational activity, and the difference in the number of lines is due mainly to the differences in relative intensities. Most vibrations are fundamental modes, and only ν_1 ($\tau(Ph-C_\alpha)$) exhibits some progressions.

Computed and experimental vibrational modes and their sequences match each other very satisfactorily, and no scaled harmonic vibrational frequencies are required, although small changes alter the order of a few vibrations (Tables 4 and 5). At the conformers' size of MPEA, the normal modes provided by the computations may be considered excellent when compared with the standard computational methods.[21] The largest vibrational wavenumber differences are found in the modes involving torsional or bending motions of the bonds $C_\alpha-C_\beta$ and/or $Ph-C_\beta$. For example, the combination of the $Ph-C_\beta-C_\alpha$ skeletal bending and the $Ph-O-CH_3$ wagging, identified as ν_4, changes in the emission spectra from 100 cm^{-1} in the CF2 F

TABLE 4: Vibrational Assignment of the MPEA Gauche Conformers[a]

origin A		identiciation CF8[b]		origin B		identification CF5		origin C		identification CF7		origin D		identification CF4	
exc	em	calc	assign	exc	em	calc	assign	exc	em	calc	assign	exc	em	calc	assign
34 m	40 s	48	ν_1	30 m	36 w	39	ν_1	31 m	41 m	50	ν_1	37 m	44 w	46	ν_1
50 vw		64	ν_2	51 vw	59 vw	62	ν_2	51 vw		64	ν_2		61 w	66	ν_2
	87 w	97	ν_3		72 vw	78	$2\nu_1$	62 m		100	$2\nu_1$		88 vw	78	$2\nu_1$
131 m	136 m	137	ν_4		101 vw	94	ν_3		89 w	98	ν_3	132 s	139 m	133	ν_4
240 m		233	ν_6	117 vw			$3\nu_1$	120 m		200	$4\nu_1$	239 s	237 w	235	ν_6
271 w	288 w	255	ν_7	131 m		135	ν_4		131 w	134	ν_4		243 w	258	ν_7
335 vw		333	ν_9	169 w	167 vw		$\nu_1 + \nu_4$	172 w	142 w	184	$\nu_1 + \nu_4$	284 m			?
378 m	380 m	381	ν_{10}		234 w	234	ν_6	238 m	230 w	233	ν_6	291 m		310	ν_8
398[c] m			?		264 w	254	ν_7	250 vw	244 w	256	ν_7	321 w		333	ν_9
403 m		410	ν_{11}		275 w	284	ν_8	309 vw		304	ν_8	377 m		360	ν_{10}
423 m	423 s	427	ν_{12}	309 w	317 w		?	376 m		375	ν_{10}	408 s	423 m	427	ν_{11}
490 m		475	ν_{13}		325 w	329	ν_9		405 m	408	ν_{11}	502 s		477	ν_{13}
505 s			?	340 vw	361 w	366	ν_{10}	500 m		475	ν_{13}	518 m	525 m	524	ν_{14}
521 m	528 s	524	ν_{14}	383 m	387 w			518 m			?	541 m			$\nu_1 + \nu_{13}$
	564 m	569	ν_{15}		414 w	421	ν_{11}	530 m		523	ν_{14}	568 m	564 m	567	ν_{15}
653 m	642 w	652	ν_{16}	485 sh	480 w	475	ν_{13}	560 m	567 m	570	ν_{15}	608 m		652	ν_{16}
697 s	696 w	707	ν_{17}	522 m	518 s	524	ν_{14}	805 vs	801 m	819	ν_{19}	804 vs		821	ν_{19}
804 vs		821	ν_{19}	540 sh	538 w		?	811 w		779	$\nu_8 + \nu_{13}$	812 vs	826 s	822	ν_{20}
823 vs	820 vs	827	ν_{20}	570 m	581 m	567	ν_{15}	820 vs	827 s	822	ν_{20}	819 vs	845 s	834	ν_{21}
838 vs	837 vs	839	ν_{21}		662 w	651	ν_{16}		844 s	835	ν_{21}	919 s	923 m	925	ν_{24}
	916 s	923	ν_{24}		706 w	707	ν_{17}		908 m	924	ν_{24}		1071 m	1071	ν_{29}
	965 m	968	ν_{26}	750 w		733	ν_{18}		1047 w	1030	ν_{28}		1189 m	1179	ν_{33}
1040 s		1030	ν_{28}	788 m	780 w	821	ν_{19}		1186 m	1179	ν_{33}		1217 s	1212	ν_{35}
	1220 s	1222	ν_{35}		804 w	826	ν_{20}		1208 s	1208	ν_{34}		1233 m	1229	ν_{37}
	1239 s	1233	ν_{36}	838 sh		840	ν_{21}		1309 s	1287	ν_{38}		1260 s	1250	ν_{38}
	1262 s	1286	ν_{37}	861 sh	851 m	858	ν_{22}						1314 m	1344	ν_{39}
	1378 m	1378	ν_{41}	884 s	878 s	887	ν_{23}								
					907 m	922	ν_{24}								
					973 w	972	ν_{26}								
					1088 m	1071	ν_{29}								
					1148 m	1143	ν_{31}								
					1186 m	1179	ν_{33}								
					1226 sh	1225	ν_{36}								
					1242 s	1233	ν_{37}								
					1292 s	1287	ν_{38}								

[a] The following abbreviations are used: Exc: Frequencies from the REMPI spectrum as identified in the HB experiment; Em: Emission frequency taken from the emission spectrum; Calc: Calculated frequencies at the B3LYP/6-31+G* level (values in cm^{-1}). [b] The description of the vibrational frequencies for CF8 is as follows: ν_1: τ(Ph−C_β); ν_2: ρ_t(Ph−O−CH_3) + δ(Ph−C_α−C_β); ν_3: τ(C_α − C_β); ν_4: ρ_w(Ph−O−CH_3) + δ(Ph−C_α−C_β); ν_6: δ(Ph−O−CH_3) + τ(C_α−N); ν_7: τ(C_α − C_β) + δ(Ph−O−CH_3); ν_8: τ(O−CH_3) + τ(C_α−C_β); ν_9: 10b;ν_{10}: 10β + τ(Ph−C_β); ν_{11}: 6a; ν_{12}: 16a; ν_{13}: 16a + δ(C_α−C_β−N); ν_{14}: 16b; ν_{15}: 16b + ρ_t($C_\alpha H_2$) + ρ_t($C_\beta H_2$); ν_{16}: 6b; ν_{17}: 4; ν_{18}: 4 + ρ_t($C_\alpha H_2$); ν_{19}: 10a; ν_{20}: 10a + ρ_t($C_\alpha H_2$); ν_{21}: 17b; ν_{22}: ρ_w(NH_2); ν_{23}: ρ_w(NH_2) + ρ($C_\beta H_2$); ν_{24}: ρ_t(NH_2) + ρ_t($C_\alpha H_2$) + ρ_t($C_\beta H_2$); ν_{26}: 17a; ν_{27}: 19a; ν_{28}: 17a; ν_{29}: σ(C_α−N) + τ(C_α−C_β); ν_{29}: σ(O−CH_3); ν_{31}: 18b; ν_{33}: ν_s(CH_3); ν_{34}: 9a; ν_{35}: ρ_w(CH_3); ν_{36}: ρ_t($C_\beta H_2$); ν_{37}: 18a;ν_{38}: 18a + ν_{as}(Ph−O−CH_3); ν_{39}: 3; ν_{40}: 3 + ρ_t(NH_2) + ρ_t($C_\alpha H_2$) + ρ_t($C_\beta H_2$); ν_{41}: 9b + ρ_w($C_\alpha H_2$). Were τ: torsion, δ: bending, ν_{as}: asymmetric stretching, ν_{as}: symmetric stretching, σ: stretching, ρ_t: twisting, ρ_w: wagging, and ρ_r: rocking. [c] Overlapped with other band.

peak to 136 cm^{-1} in the CF8 A peak. The vibrational frequency differences between gauche and trans conformers are due mainly to the interaction between the NH_2 group and the aromatic ring, which in the gauche conformers hinders the movements of the Ph−C_β-C_α skeletal.

Neither the gauche nor the anti conformers' spectra show ν_5 (τ(O−CH_3)) and ν_{25} (17a for anti and 17a + ρ_w(NH_2) for gauche) vibrational modes. In addition, the anti spectra lack some vibrations, mainly related to the aromatic ring, the most noticeable being the ν_{13} (≡6a[18]), which usually appears as a strong peak in benzene derivatives' spectra. In the gauche conformers' spectra, this band (ν_{11}) is a medium-intensity peak. Other aromatic ring vibrations not found in the anti spectra, but which appear in the gauche ones, are $\nu_{18} \equiv$ 19a, $\nu_{27} \equiv$ 18a, and $\nu_{31} \equiv$ 18b. As observed, they are both in-plane and out-of-plane vibrations. No pattern of behavior is found in the absence of these vibrations, which may be due to the F and G peaks' small intensity or to overlapping with other strong bands.

The strongest bands in the spectra are those related to modes 10a (ν_{19} for the gauche and ν_{20} for the anti) and combinations of 10a with skeletal vibrations (see Tables 4 and 5). These vibrations have intensities similar to those of conformers' 0_0^0 bands in the REMPI spectrum, but they are less intense in the R2PI spectrum.

Finally, it is worth noting that, as a general trend, there are few or no appreciable differences between the ground and the excited states' vibrational frequencies, and their agreement with the calculated values at the B3LYP/6-31+G* level is excellent.

C. Conformer Stability. The nine conformers' energy differences are due to two interactions of different sign: the unfavorable interaction between the NH_2, $C_\alpha H_2$, and $C_\beta H_2$ hydrogens appearing in the CF2−CF8 structures, and the stabilizing HN−H···π interaction. In the absence of the latter interaction, the most stable conformation is CF1, as the skeletal hydrogens are as far apart as geometry permits. A rotation of the C_α−N bond leads to an interaction between the NH_2 and $C_\alpha H_2$ hydrogens, and consequently, CF2 and CF3 are ca. 70 cm^{-1} less stable than CF1 at the B3LYP/6-31+G* level, and 21 and 38 cm^{-1} less stable respectively, at the B3LYP/6-311+G* level. The energy difference between CF2 and CF3 is ca. 16 cm^{-1} (Table 2) and can be originated only by the asymmetry imposed on the molecule by the O(Me) group. The

TABLE 5: Vibrational Assignments of the MPEA Folded Anti Conformers[a,b]

origin E		identification CF1		origin F		identification CF2		origin G		identification CF3	
exc	em	calc	assign	exc	em	calc	assign	exc	em	calc	assign
53 m		62	ν_2	26 m	37 m	34	ν_1	56 w		63	ν_2
65 vw		70	$2\nu_1$	47 w		68	$2\nu_1$	124 m		131	$\nu_1+\nu_3$
125 s		129	$\nu_1+\nu_3$	59 m	76 m	62	ν_2	229 vw		229	ν_6
	139 m	138	$\nu_1+\nu_4$	88 s		91	ν_3	236 m		248	ν_7
187 m		193	ν_5		100 m	103	ν_4		354 w	354	ν_{10}
239 m	242 vw	259	ν_7	270 m		261	ν_8	526 m		531	ν_{14}
341 m	342 w	352	ν_{10}		319 w	318	ν_9	570 m	568 m	570	ν_{15}
371 m		358	ν_{11}	350 w		352	ν_{10}	821 m		821	ν_{20}
376* s		386	$2\nu_5$	385 w		387	ν_{11}	829 s		838	ν_{21}
397 s	389 vw	387	$\nu_1+\nu_{10}$	534 w		531	ν_{14}	835 s		850	ν_{22}
	413 m	427	ν_{12}		566 m	569	ν_{15}		862 s	864	ν_{23}
500 s			?	611 s					1264 m	1271	ν_{37}
517 s			?		642 w	653	ν_{16}		1410 m	1430	ν_{43}
524 w	528 m	531	ν_{14}		825 m	822	ν_{20}				
568 s	573 m	568	ν_{15}		854 s	850	ν_{22}				
	652 m	653	ν_{16}		890 m	864	ν_{23}				
	717 m	720	ν_{17}		1300 w	1328	ν_{39}				
807 vs		821	ν_{20}								
813 vs	825 vs	834	ν_{21}								
818 vs	847 vs	850	ν_{22}								
919 s	930 m	942	ν_{24}								
	1063 m	1071	ν_{29}								
	1199 m	1179	ν_{33}								
	1222 s	1231	ν_{36}								
	1266 m	1286	ν_{37}								
	1321 s	1322	ν_{39}								
	1633 m	1626	ν_{51}								

[a] The following abbreviations are used: Exc: Frequencies from the REMPI spectrum as identified in the HB experiment; Em: Emission frequency taken from the emission spectrum; Calc: Calculated frequencies at the B3LYP/6-31+G* level (values in cm^{-1}). [b] ν_1: $\tau(Ph-C_\beta)$; ν_2: $\rho_t(Ph-O-CH_3) + \delta(Ph-C_\alpha-C_\beta)$; ν_3: $\tau(C_\alpha-C_\beta)$; ν_4: $\rho_w(Ph-O-CH_3) + \delta(Ph-C_\alpha-C_\beta)$; ν_6: $\delta(Ph-O-CH_3) + \tau(C_\alpha-N)$; ν_7: $\tau(C_\alpha-N)$; ν_8: $\tau(O-CH_3)$ (for C2 ν_7 and ν_8 are interchanged); ν_9: 6a + $\delta(C_\alpha-C_\beta-N)$ [for C2 ν_9: $\sigma(C_\alpha-N)$]; ν_{10}: $\delta(O-CH_3) + \rho_r(C_\beta H_2)$; ν_{11}: $\rho_w(Ph-O-CH_3) + \delta(Ph-C\alpha-C_\beta)$; ν_{12}: 16a; ν_{14}: 16b; ν_{15}: 16b + 6a + $\delta(O-CH_3)$; ν_{16}: 6b; ν_{17}: 4 (C2 ν_{17}: 17b); ν_{20}: 10a; ν_{21}: 10a + $\delta(NH_2)$; ν_{22}: 10a + $\rho_w(NH_2)$ + $\nu_{as}(Ph-C\alpha-C_\beta)$; ν_{23}: 6a + $\rho_w(NH_2)$ + $\rho(CH_2)$; ν_{24}: 5; ν_{29}: $\sigma(O-CH_3)$; ν_{33}: $\rho_r(CH_3)$; ν_{36}: 18a + $\sigma(Ph-C_\beta)$; ν_{37}: 18a + $\nu_{as}(Ph-O-CH_3)$ + $\rho_w(CH_3)$; ν_{39}: $\rho_w(C\alpha H_2) + \rho_w(C_\beta H_2)$; ν_{43}: $\rho_t(NH_2) + \rho_w(C_\beta H_2)$; ν_{51}: 8b. Where τ: torsion, δ: bending, ν_{as}: asymmetric stretching, ν_{as}: symmetric stretching, σ: stretching, ρ_t: twisting, ρ_w: wagging, and ρ_r: rocking. [c] Overlapped with other band.

energy difference is due to a direct interaction either between O(Me) and NH_2 dipoles or through the modulation imposed on the ring by the distant methoxy group. In the same way, the energy differences between pairs of gauche conformers result from the interaction between the NH_2 group and the different (nonequivalent) sides of the aromatic ring, modulated by the O(Me) group.

When the alkylic group adopts a folded configuration by rotation on the $C_\alpha-C_\beta$ bond, an unfavorable interaction between C_α and C_β hydrogens appears. According to the calculations, this interaction is overcompensated in CF5 and CF8 structures by the $HN-H\cdots\pi$ interaction, and only partially compensated in CF4 and CF7 (see Table 2). To maximize this interaction, the $Ph-C_\beta$ bond also rotates, trying to diminish the $N-H\cdots C_1$ distance as much as possible. Although the B3LYP method can underestimate the magnitude of the interaction, the real importance of the $HN-H\cdots\pi$ interaction cannot be estimated simply by looking at the conformer's energy relative to CF1, because the difference in the conformer's relative stability is the difference between the $HN-H\cdots\pi$ interaction and that of the skeletal hydrogens. The explicit introduction of ZPE energies does not significantly affect the relative conformers' stability, although it actually increases the energy differences between some of them.

The relatively low stability of the CF6 and CF9 structures also is due to the addition of two interactions, that of the nitrogen lone pair and that of the aromatic ring electron density, to the aforementioned interaction between skeletal hydrogens. The sum of both contributions (over 500 cm^{-1}) is large enough to make the population of these conformers in the expansion beam negligible.

V. Conclusions

A study of the *p*-methoxyphenethylamine conformations in supersonic jet expansions has been conducted, by a combination of experimental (LIF, REMPI, R2PI, and dispersed emission) and theoretical calculations (B3LYP with two basis sets, 6-31+G* and 6-311+G*). As a result, the structural assignment of the seven MPEA conformers and the most prominent vibrational bands have been identified. In the assignment, the IE studies and the comparison between experimental and calculated frequencies have played an important part. Arguments based on the comparison between the relative intensities of the 0_0^0 bands have proved useless, as the interaction between the NH_2 group and the aromatic ring perturbs the transition dipole moment and therefore, the transition oscillator strength.

Of the nine possible conformers, only seven are formed: three anti and four gauche. The two absent conformers are two gauche with a destabilizing interaction between the NH_2 lone pair and the π-system electron density. The most stable conformers are the gauche, with the largest $HN-H\cdots\pi$ interaction, followed by the most stable anti. The modulation in the aromatic ring introduced by the methoxy group has a small but noticeable influence on the conformers' relative stability, leading to differences of 20 to 40 cm^{-1} for pairs of gauche conformers and between CF2 and CF3.

The most prominent features in the spectra are the 10a vibrational mode and its combinations with other skeletal

vibrations (especially NH_2 vibrations). At the same time, it is interesting to point out the absence of the 6a vibrational mode in the spectra of the anti conformers, despite its common existence as a strong feature in the benzene derivatives.

Acknowledgment. We acknowledge the grants and complimentary support from the DGES (PB91-0510, PB95-0510, and PB96-1472), the Basque Government, and the UPV, and the award of a DGES personal contract to J.A.F. I.U. and A.L. thank the Basque Government for the award of their studentships. We also appreciate the discussions and advice on theoretical computations of Prof. M. Yañez (UAM, Spain) and the discussions of experimental matters with Prof. R. B. Donovan (Edinburgh, U.K.).

References and Notes

(1) Mathews, C. K.; van Holde, K. E. *Biochemistry*, 2nd ed.; Benjamin/Cummings: New York, 1996.

(2) Martinez, S. J., III; Alfano, J. C.; Levy, D. H. *J. Mol. Spectrosc.* **1993**, *158*, 82.

(3) Martinez, S. J., III; Alfano, J. C.; Levy, D. H. *J. Mol. Spectrosc.* **1989**, *137*, 420.

(4) Phillips, L. A.; Levy, D. H. *J. Phys. Chem.* **1986**, *90*, 4921.

(5) Phillps, L. A.; Levy, D. H. *J. Chem. Phys*. **1988**, *89*, 85.

(6) Peteneau, L. A.; Levy, D. H. *J. Chem. Phys*. **1988**, *92*, 6554.

(7) Martinez, S. J., III; Alfano, J. C.; Levy, D. H. *J. Mol. Spectrosc.* **1991**, *145*, 100.

(8) Martinez, S. J., III; Alfano, J. C.; Levy, D. H. *J. Mol. Spectrosc.* **1992**, *156*, 421.

(9) Godfrey, P. D.; Hatherley, L. D.; Brown, R. D. *J. Am. Chem. Soc.* **1995**, *117*, 8204.

(10) Sun, S.; Bernstein, E. R. *J. Am. Chem. Soc*. **1996**, *118*, 5086.

(11) Dickinson, J. A.; Hockridge, M. R.; Kroemer, R. T.; Robertson, E. G.; Simons, J. P.; McCombie, J.; Walker, M. *J. Am. Chem. Soc*. **1998**, *120*, 2622.

(12) Urban, J. J.; Cronin, C. W.; Roberts, R. R.; Famini, G. R. *J. Am. Chem. Soc*. **1997**, *119*, 12292.

(13) Hockridge, M. R.; Knight, S. M.; Robertson, E. G.; Simons, J. P.; McCombie, J.; Walker, M. *Phys. Chem. Chem. Phys.* **1999**, *1*, 407.

(14) Zwier, T. S. *Annu. Rev. Phys. Chem.* **1996**, *47*, 205; and references therein.

(15) Taylor, A. G.; Bürgi, T.; Leutwyler, S. In *Jet Spectroscopy and Molecular Dynamics*; Hollas, J. M., Phillips, D., Eds.; Blackie: London, 1995; Chapter 5; and references therein.

(16) Longarte, A.; Fernández, J. A.; Unamuno, I.; Castaño, F. *J. Chem. Phys.* **2000**, *112*, 3170.

(17) Rauhut, G.; Pulay, P. *J. Phys. Chem.* **1995**, *99*, 3093.

(18) Frisch, M. J.; Trucks, G. W.; Schlegel, H. B.; Scuseria, G. E.; Robb, M. A.; Cheeseman, J. R.; Zakrzewski, V. G.; Montgomery, J. A., Jr.; Stratmann, R. E.; Burant, J. C.; Dapprich, S.; Millam, J. M.; Daniels, A. D.; Kudin, K. N.; Strain, M. C.; Farkas, O.; Tomasi, J.; Barone, V.; Cossi, M.; Cammi, R.; Mennucci, B.; Pomelli, C.; Adamo, C.; Clifford, S.; Ochterski, J.; Petersson, G. A.; Ayala, P. Y.; Cui, Q.; Morokuma, K.; Malick, D. K.; Rabuck, A. D.; Raghavachari, K.; Foresman, J. B.; Cioslowski, J.; Ortiz, J. V.; Stefanov, B. B.; Liu, G.; Liashenko, A.; Piskorz, P.; Komaromi, I.; Gomperts, R.; Martin, R. L.; Fox, D. J.; Keith, T.; Al-Laham, M. A.; Peng, C. Y.; Nanayakkara, A.; Gonzalez, C.; Challacombe, V.; Gill, P. M. W.; Johnson, B.; Chen, V.; Wong, M. W.; Andres, J. L.; Gonzalez, C.; Head-Gordon, M.; Replogle, E. S.; Pople, J. A. GAUSSIAN 98, revision A.3; Gaussian Inc.: Pittsburgh, PA, 1998.

(19) Fernández, J. A.; Bernstein, E. R. *J. Chem. Phys.* **1997**, *106*, 3029.

(20) Wilson, E. B. *Phys. Rev.* **1934**, *45*, 706.

(21) Ferraro, J. R.; Ziomek, J. S. *Introductory Group Theory*, 2nd ed.; Plenum Press: New York, 1975.